

# 1

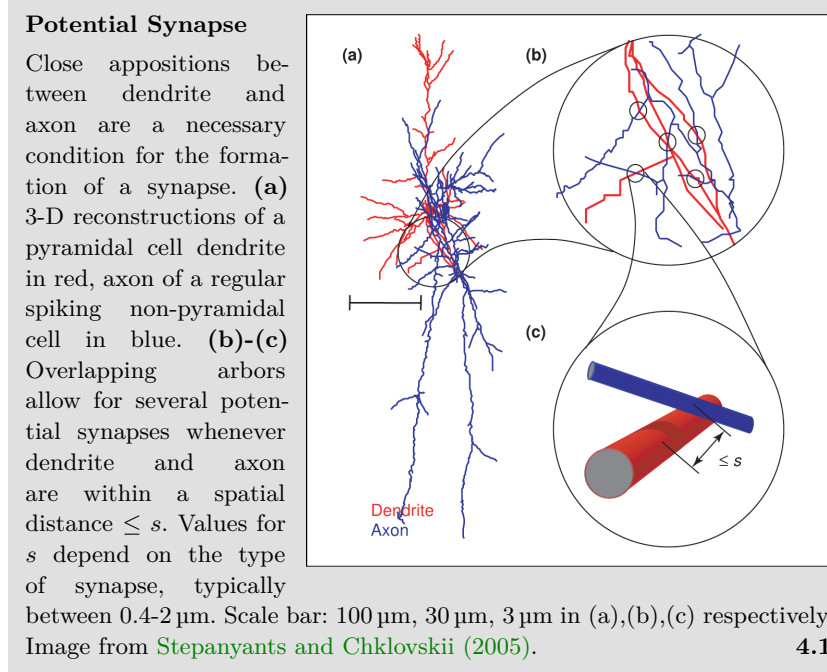
## NETWORK MODEL

---

Referring to anisotropic characteristics in local cortical circuits of the rat's brain, a network model implementing anisotropic tissue geometry is developed. The introduction of a rewiring algorithm and qualitative anisotropy measure lay the foundation for the analysis of structural aspects of this model in Chapter ??.

### 1.1 ANISOTROPY IN NEURAL CONNECTIVITY

Neurogeometry addresses the problem of inferring synaptic connectivity from the geometric shapes of axon and dendrites. A fundamental concept in this field is that of a *potential synapse* (Stepanyants et al. 2002). Defined as the potential axonal-dendritic connection of two neurons, present whenever the axon of one neuron is within a spatial distance  $s$  of the dendrite of the other, it is a necessary, although not sufficient, condition for the formation of a synaptic connection (Figure 1.1). The existence of such close appositions solely depends on dendritic and axonal anatomy; identification of defining morphological characteristics in both axon and dendrite would therefore allow for a model of local network connectivity, assuming for example that a certain ratio  $r$  of potential synapses turn into active contacts independently. It is the hope that such a model, motivated from the geometry of a neuron's functional compartments, not only displays inherent patterns of connectivity similar to what has been observed in biological networks, but also proofs itself as a testing ground for how this connectivity may affect network dynamics.



high variability in  
axonal  
morphology

Finding stereotypical anatomical characteristics however is difficult, as axonal morphology is, in general, highly diverse (Debanne 2004). Across different species, distinct regions in the central nervous system and different neuron types, axons display a wide variety of shapes characterized by morphometric parameters such as total length, branching complexity and axonal extent (Ropireddy et al. 2011). Typical exam-

ples of distinct morphology include the T-shaped axons of cerebellar granule cells branching only at a singular point (Ramon and Cajal 1911), and axons of hippocampal CA3 pyramidal cells, which, in stark contrast, may feature up to 40 branches resulting in a total length of axon collaterals of up to 12 mm (Ishizuka et al. 1990).

It is therefore imperative to confine this analysis to a specific brain region and neuron type. In this study, we set the focus on circuits of pyramidal cells in the mammalian cortex. More specifically, local circuits of thick tufted layer V pyramidal neurons in the rat's somatosensory cortex have been the target of advanced experimentation (Song et al. 2005; Perin et al. 2011; Romand et al. 2011; Ramaswamy et al. 2012), and will serve as a benchmark for results in neural morphology and network connectivity in this report.

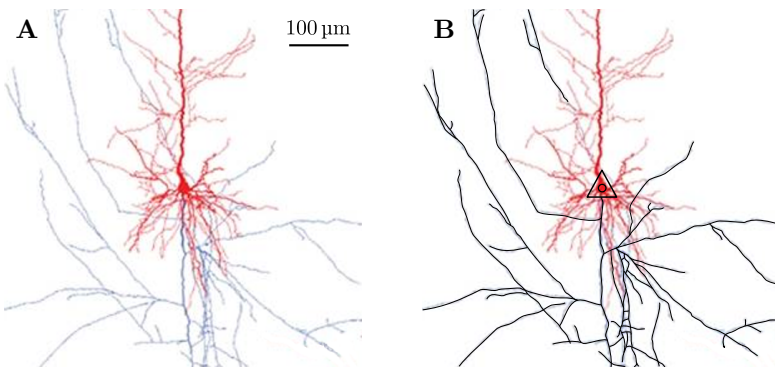


**Figure 1.2: Tracing axonal branching of a pyramidal cell** In a 3-D model reconstructed from biocytin-labeled thick-tufted layer V pyramidal cells in the somatosensory cortex of postnatal (day 14) Wistar rats, Romand et al. (2011) depict dendritic compartments in red, axonal compartments in blue. **A)** A 600  $\mu\text{m}$  window centered on the soma of the pyramidal cell shows the main stem of the cell's axon projecting downwards in a straight line, collaterals branching at various angles. **B)** Using image manipulation software, axon morphology was manually traced and is emphasized in black.

Axonal morphology of pyramidal cells in the cerebral cortex is well described. From the soma the single main stem of the axon originates and projects downwards, describing a trajectory closely resembling a straight line (Braitenberg and Schüz 1998). At arbitrary points along this path, collaterals branch off at various angles and constitute themselves linear paths until they further ramify or terminate. Displaying a high degree of ramification, axonal trees of cortical pyramidal cells build, in general, complex structures (Petersen et al. 2003; Ramaswamy et al. 2012). Cortical slice experiments analyzing neural anatomy are typically constrained by a slice thickness of 300  $\mu\text{m}$ . On this scale, 3-D reconstruction from labeled thick tufted layer V pyramidal cells reveals

cortical axons  
form straight lines,  
arborize profusely

characteristic morphology of the axonal tree (Figure 1.2). The downwards projecting, straight axon branches at several points, forming collateral branches that travel in linear path as well.

In a statistical view, this characteristic axonal morphology results in high axon branch densities along the main stem, whereas distant regions display a relatively low density (Figure 1.3). Specifically, axon collaterals do not cluster around the soma but align with the main stem's projection. As presence of an axonal branch constitutes a necessary condition for a potential synapse, a higher concentration of potential and, subsequently, realized synapses is expected in regions of high branch density. For a coherent picture of local connectivity profiles, however, dendritic morphology needs to be considered as well.

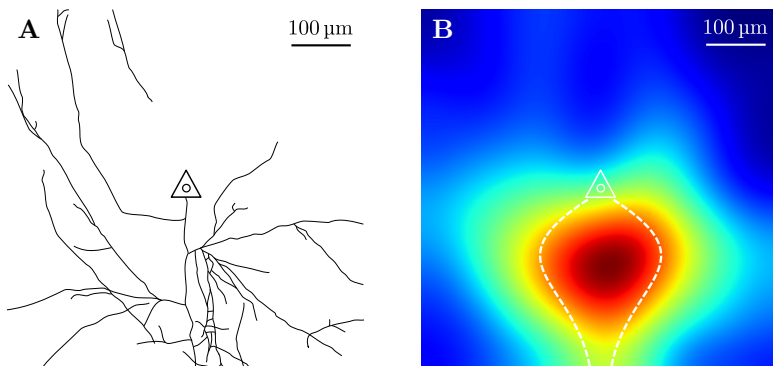


**Figure 1.3: Illustrating axonal branch density** In a sample of 5 reconstructions from thick-tufted layer V pyramidal cells (Romand et al. 2011), tracing axonal morphology illustrates characteristic branch density along the axon's main stem. **A)** Example of extracted axonal tree. Outline manually traced using image manipulation software. Soma indicated by triangle. Original data from Romand et al. (2011). **B)** Overlaying 5 axonal trees extracted as in A), applying a Gaussian filter and displaying high axon densities in warm colors, illustrates the characteristic higher branch densities along the axon's main stem.

*basal dendrites dominate local connectivity*

Dendritic anatomy of cortical pyramidal cells is inherently bipartite. From the soma several *basal dendrites* emerge and extend into arbitrary directions, branching profusely until they terminate. The single *apical dendrite* emerges from the apex of the pyramidal cell and ascends in a linear trajectory, forming occasional collateral branches until finally terminating into the apical tuft, where the dendrite branches several times to form a tree like structure (Feldman 1984). On the scale of typical cortical slice thickness, however, the apical dendrite is cut off and the basal dendrite dominates the dendritic morphology and potential of dendritic-axonal connections (Figure 1.4). The radial extension of dendritic branches results in a high concentration of dendritic branches

around the soma, much in the contrast to the findings of axonal branch densities before.

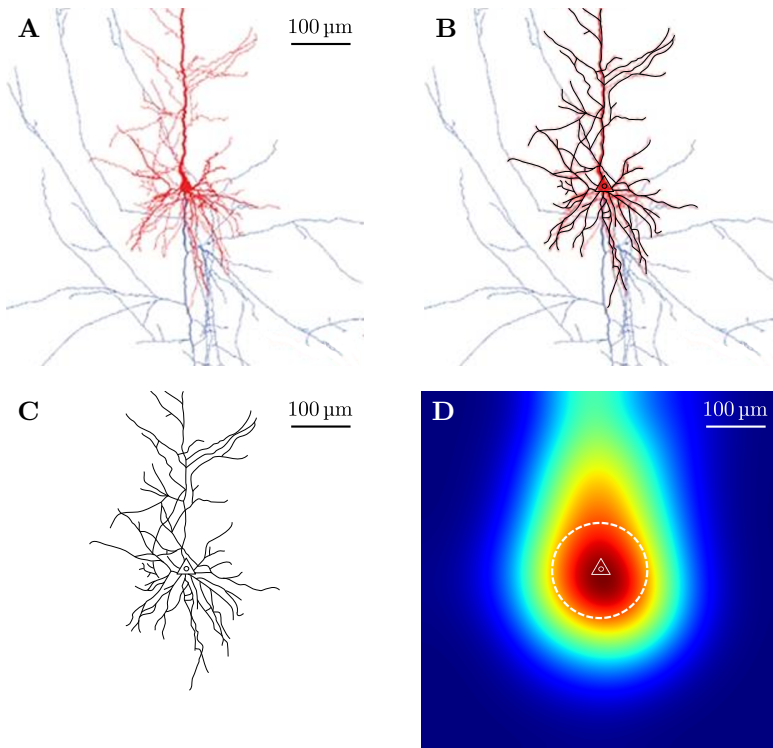


**Figure 1.4: Dendritic morphology and branch density** Using neuronal morphology of thick-tufted layer V pyramidal cells recorded by Romand et al. (2011), dendritic anatomy is traced and combined to illustrate high branch density around the soma. **A)** In a 600  $\mu\text{m}$  window centered on the soma, basal dendrites (red) are visible extending around the soma. The ascending thick apical dendrite (red) is cut off and apical tuft is not shown. **B)-C)** Manual tracing of dendritic outlines in five samples (one shown), allows for clearer identification of stereotypical morphology and later analysis. **D)** Combining 5 dendritic outlines as shown in C) and subsequent Gaussian filtering reveals the relatively high dendritic branch density around the soma.

Combining the above results of dendritic and axonal branch densities in the light of neurogeometry, a clear concept of anisotropy of neural connectivity emerges. As dendritic branches of potential post-synaptic targets extend radially from the soma and do not display a preferred direction, target neurons for outgoing synaptic contacts originating from a single pyramidal cell, cluster around the downwards projecting axon (Figure 1.5). In their in-depth study, Stepanyants and Chklovskii (2005) confirm the overrepresentation of potential synapses along the axon for pyramidal cells. Consistent with the notion that stereotypical morphology of pyramidal cells is intrinsic to the local network's connec-

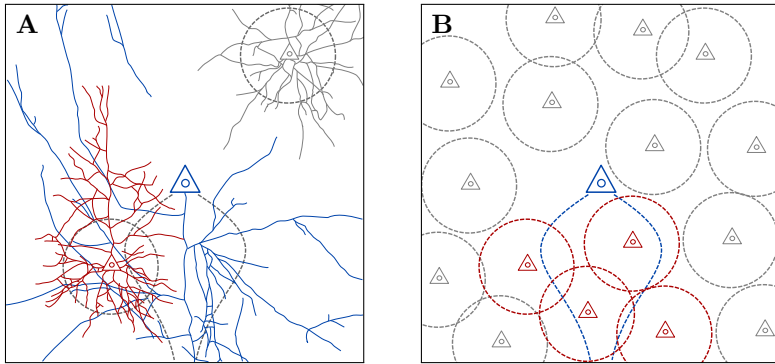


**Figure 1.5: Connected neurons of a single pyramidal cell align with axonal projection** Reducing the full axonal (blue, cf. Figure 1.2) and dendritic trees (red, gray, cf. Figure 1.4) as shown for two neurons in A) to their stereotypical axonal (blue) and dendritic profiles (red, gray) in B), demonstrates how connected neurons (red) tend to cluster around the pre-synaptic axon’s profile, as spatial closeness constitutes a necessary condition for the formation of contacts. Unconnected neurons (gray) are found distant from the axon’s projection, but not necessarily distant from the soma.

tivity profile, they also find that anisotropy of this degree is *not* present in spiny stellate neurons located in lower-layer-4.

## 1.2 ANISOTROPIC GEOMETRIC NETWORK MODEL

In this section we formulate a model of network connectivity incorporating anisotropy as outlined in the last section. A

With this in mind, we propose the following model: On a square surface of side length  $s$ , a number of  $N$  point neurons are randomly, uniformly distributed. Connected neighbors are then calculated for each neuron separately and independently, by determining the randomly, uniformly distributed direction of the neuron’s single axon. In this direction the axon traverses over the surface describing a straight path, terminating only when an edge of the surface is reached. Directed contacts are made with every neuron that is within a width  $w(x)$  of the axon’s trajectory, where in general  $w$  depends on the axon length  $x$  at this point (Figure 1.6).

random axonal orientation yields relevant connectivity

The implementation of arbitrary axonal orientation is crucial to the model. Although cortical axons are described as consistently projecting downwards (Braitenberg and Schüz 1998, cf. Section 1.1), combining exclusively vertically aligned axons with the simplified axonal and dendritic morphological profiles would result in a “vertically staggered

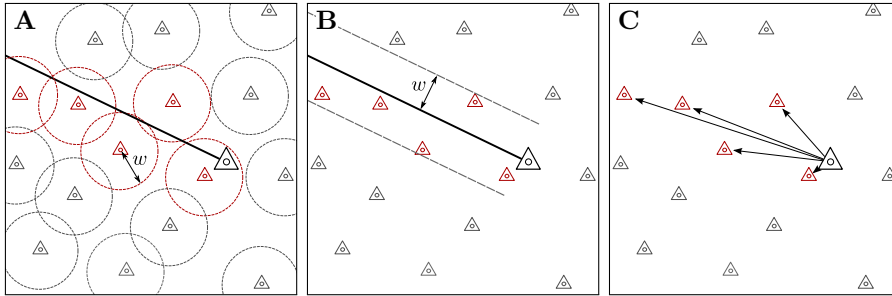


**Figure 1.6: Anisotropic geometric network model and interpretations of width parameter  $w$**  Illustrating the process of finding connections for one neuron (large triangle, black), the axon describes a linear trajectory in an arbitrary direction and until terminating on the surface's edge. Target neurons (red) are encountered along the path within a distance  $w$ , which is in **A**) interpreted as a dendritic radius or, equivalently, in **B**) as a “bandwidth” of the axon. Connections to the encountered targets are then established as projections in **C**), consistent with the directed nature of synapses in biological networks (cf. Chapter ??).

connectivity” - neurons could then only project to targets located below them. It is in fact not a vertical alignment of axon orientation, but the anisotropy in neural connectivity - the observation of neuronal targets aligning with the axonal projection - that we try to capture and analyze in this model.

We will refer to the model as the *anisotropic geometric network model*. Trying to provide a simple, abstract model isolating anisotropy in connectivity, in most of this study the width  $w$  is assumed to be constant, a notable exception being the exploration in ???. In the graph theoretic context the anisotropic network model is a random graph model, in which a realization of the random process results in a geometric directed graph with a special mode of connectivity. We can formally define such realization as:

**Definition 1.1** (Anisotropic geometric graph). Let  $n \in \mathbb{N}$  and  $w \in (0, \infty)$ . An *anisotropic geometric graph*  $G_{n,w}$  then consists of a tuple  $(G, \Phi, a)$ , of a simple directed graph  $G$  with  $|V(G)| = n$  vertices and the maps  $\Phi : V(G) \rightarrow [0, 1]^2$  and  $a : V(G) \rightarrow [0, 2\pi)$ , such that for every vertex pair  $v, v' \in V(G)$  and edge  $e \in E(G)$  with  $s(e) = v$  and  $t(e) = v'$  exists if and only if the inequalities

$$R_{-a(v)} (\Phi(v') - \Phi(v)) \hat{e}_x \geq 0 \quad \text{and} \quad |R_{-a(v)} (\Phi(v') - \Phi(v)) \hat{e}_y| \leq \frac{w}{2}$$

hold. Here  $R_\varphi$  is the rotation matrix of angle  $\varphi$  in the Cartesian plane and  $\hat{e}_x, \hat{e}_y$  are the standard unit vectors.

The anisotropic random graph model then is then giving the probability distribution over the set of anisotropic random graphs by describing a random process generating such graph.

**Definition 1.2** (Anisotropic random graph model). Let  $n \in \mathbb{N}$  and  $w > 0$ . The *anisotropic random graph model*  $G(n, w)$  is a probability space over the set of anisotropic geometric graphs with a probability distribution induced by the following process: Let  $G$  be an empty graph with  $n$  vertices. Assign randomly and uniformly to every vertex  $v \in V(G)$  a position  $\Phi(v) \in [0, 1]^2$  and axonal orientation  $0 \leq a(v) < 2\pi$ . Then add edges such that  $(G, \Phi, a)$  is an anisotropic geometric graph  $G_{n,w}$ .

*anisotropic model  
is scale-free*

As with every geometric graph model introduced, we restrict the surface to be the unit square. This does not limit the model, as only the relative width of the axon band in regard to the surface's side length is determining connectivity statistics - the expected number of connections is easily obtained by the quotient of the area covered by the axon and the surface area, making connectivity statistics in the anisotropic random graph model scale-free.

This study of anisotropic geometric graphs. To enable this analysis, some prior work which composes the rest of this chapter. Integral to our is a numerical implementation of the model.

### 1.3 NUMERICAL IMPLEMENTATION

Numerical implementation of the anisotropic random graph model was achieved in Python<sup>1</sup>. Relying on the NumPy for mathematical as part of the scientific library ([Jones et al. 2001–](#)) and graph tool, a graph manipulation ([Peixoto 2014](#)), convenience as well as potency could be secured.

The algorithm for the generation of anisotropic networks, closely resembles the Definition 1.1.

*determine  
parameter set to  
generate sample  
graphs*

To harness the numerical implemenation to generate networks, a set of parameters needs to be chosen. The network size  $N$  strongly influences the needed computational efforts in calculations based on the generated graphs and has thus been set to  $N = 1000$ . Choosing the surface side-length arbitrarily as  $s = 100$ , the axon width  $w$  determines connectivity in the network, the relation between width  $w$  and overall connection

---

<sup>1</sup> Python Software Foundation. Python Language Reference, version 2.7. Available at <http://www.python.org>

probability  $p$  being shown in [Figure 1.7](#). In their analysis of connectivity of thick-tufted layer V pyramidal cells in neonatal rats (day 14), [Song et al. \(2005\)](#) report an overall connection probability of  $p = 0.116$ , consistent with prior reports of a cortical connection probability of  $p \approx 0.1$ . Choosing  $w$  to be constant, we determine the axon width such that overall connectivity matches the value report by Song et al. and obtain  $w = 12.6$  ([Figure 1.7](#)).

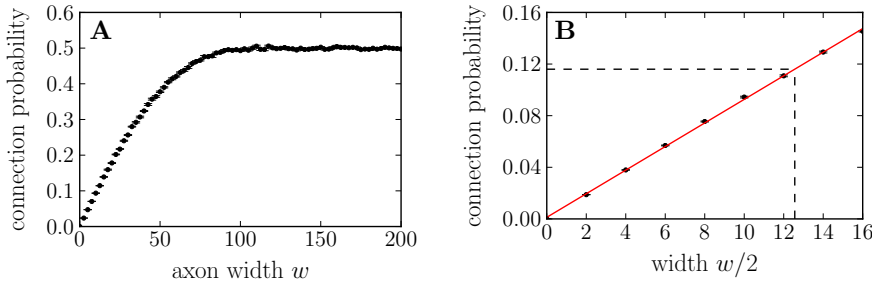


**Figure 1.7: Axon width dependent connection probability determines parameter for numerical analysis** Generating anisotropic networks with different axon widths  $w$  and extracting probability  $p$  of directed connection between two random nodes, demonstrates the dependency of  $p$  on the width parameter  $w$ . **A)** At an axon width of over  $w = 100$ , exceeding the square's side length, the connection probability saturates at  $p = 0.5$ , as axon bands are essentially “cutting” the square in a connected and unconnected half (c5b64f3e). **B)** For small  $w$  the connection probability is a linear function of  $w$ , allowing the width  $w_S/2$  at which  $p(w_S) = 0.116$  to be determined by a linear fit as  $w_S/2 = 12.6$  (585a946f).

Having determined parameters... With this parameter set we generate a sample of 25 graphs

## 1.4 DISTANCE DEPENDENT CONNECTIVITY

random graph  
models in  
Section ??

In Gilbert's random graph model  $G(n, p)$ , probability of connection  $p$  is independently chosen and a fixed value for all vertex pairs. The anisotropic geometric graph model introduced in Section 1.2 is itself a random graph model - node positions as well as preferred directions of connection are uniformly at random distributed. In contrast to Gilbert's model however, neither is the probability of connection between a given vertex pair independent of the realization of other edges in the graph, nor is it a fixed value - probabilities strongly depend on internode distance in the anisotropic geometric graph model introduced.

Analyzing dependencies in the anisotropic model, specifically by identifying prevalent patterns of connectivity and relating these modes of non-randomness to biological findings, is the main focus of Chapter ?. However, such structural correlations may not necessarily be an inherent feature of the network's anisotropy - distance dependent connectivity alone, as imposed by the model's specific geometry, may be the cause for emerging dependencies. It is therefore a crucial initial task to map the anisotropic model's distance dependent connection probability. Inferring connection probability as a function of internode distance and comparing it with computational results, in this section we explore distance connectivity of the anisotropic network model, securing a vital component in the analysis of structural features.

**Theorem 1.3.** *Let  $(G, \Phi, a)$  represent an arbitrary realization of the anisotropic random graph model  $G(n, w)$ . Define  $C : [0, \sqrt{2}] \rightarrow [0, 1]$  as the distance-dependent connection probability profile of  $(G, \Phi)$ , that is such that  $C(x)$  is the probability that for a vertex pair  $(v, v') \in V(G)^2 \setminus \Delta_{V(G)}$  in distance  $x = \|\Phi(v) - \Phi(v')\|$  the vertex  $v$  projects to vertex  $v'$ . Then*

$$C(x) = \begin{cases} \frac{1}{2} & \text{for } x \leq w/2 \\ \frac{1}{\pi} \arcsin\left(\frac{w}{2x}\right) & \text{for } x > w/2. \end{cases}$$

*Proof.* Let  $v, v'$  be a pair of vertices in  $V(G)^2 \setminus \Delta_{V(G)}$  in Euclidean distance  $x$  of each other. The vector difference  $\Phi(v') - \Phi(v)$  may then be written as  $xe^{i\theta}$ , with  $0 \leq \theta < 2\pi$ . We have

$$R_{-\alpha(v)} xe^{i\theta} = xe^{i(\theta - \alpha(v))}.$$

Only for suitable combination of  $\theta$  and  $\alpha(v)$  an edge from  $v$  to  $v'$  exists. Assuming  $\alpha(v)$  fixed, we calculate the probability of connection depending on the random choice of  $\theta$ . We can assume  $\alpha(v) = 0$ , otherwise the same argument holds for  $\theta' = \theta - \alpha(v)$ .

From 1.1 we obtain the necessary and sufficient conditions

$$x \cos \theta \geq 0 \quad \text{and} \quad |x \sin \theta| \leq \frac{w}{2}.$$

Choosing uniformly at random  $\theta$  in the range of  $[0, 2\pi)$ , the first condition is satisfied with a probability of  $\frac{1}{2}$ . Consider for the second condition  $\theta \in [0, \pi)$ . We have

$$\sin \theta \leq \frac{w}{2x},$$

and for  $x \leq \frac{w}{2}$  the inequality holds for all  $\theta$  by definition of  $\sin \theta$ . In the case of  $x > \frac{w}{2}$ , we note that for the first condition to hold  $\theta$  must already be in  $[0, \frac{\pi}{2})$  and can thus write the second condition  $\theta$  as

$$\theta \leq \arcsin \frac{w}{2x},$$

yielding  $C(x)$  by combining the considerations above and using the symmetry of sine for  $\theta$  in the third and fourth quadrant.  $\square$

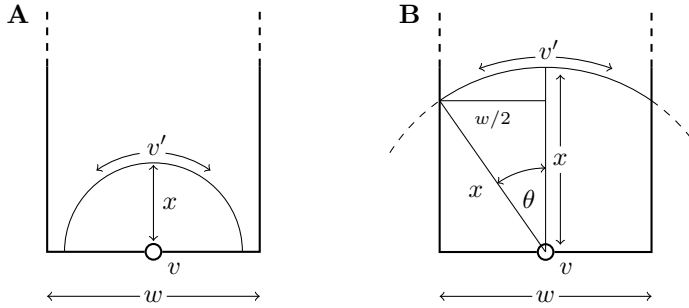


**Figure 1.8: Illustrating the proof of Theorem 1.3** Distance-dependent connectivity profile  $C(x)$  in an anisotropic geometric graph calculated from geometric dependencies. **A)** In the case of  $x \leq w/2$ , target  $v'$  may be located anywhere on the shown semicircle and therefore receives input from  $v$  with probability  $1/2$ . **B)** For  $x > w/2$ , suitable positions for target  $v'$  are dependent on  $x$ . The geometric relation  $\sin \theta = w/2x$  leads to the distance-dependent connectivity profile as described in Theorem 1.3.

We can verify this result by computationally extracting the distance dependencies in the sample graphs generated.

Create additionally a new distance depenedent network sample graphs and great!

## 1.5 REWIRING

It is in our highest interest to compare results to. To this end we intro-

*eliminate  
anisotropy  
through rewiring*

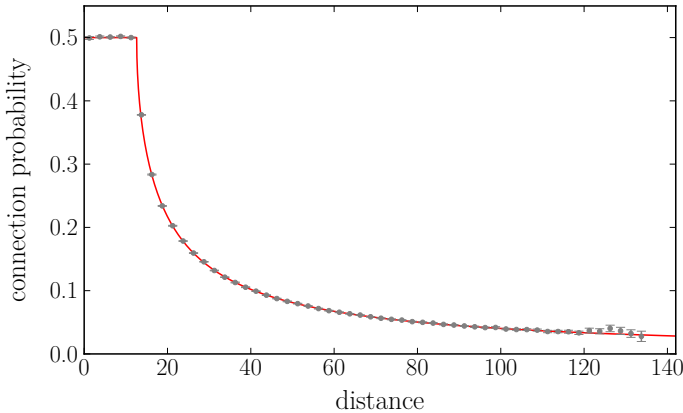


**Figure 1.9: Predicted distance-dependent connection probability profile is matched by numerical computation** In a 3-D model reconstructed from biocytin-labeled thick-tufted layer V pyramidal cells in the somatosensory cortex of postnatal (day 14) Wistar rats, Romand et al. (2011) depict dendritic compartments in red, axonal compartments in blue. **A)** A 600  $\mu\text{m}$  window centered on the soma of the pyramidal cell shows the main stem of the cell's axon projecting downwards in a straight line, collaterals branching at various angles. **B)** Using image manipulation software, axon morphology was manually traced and is emphasized in black.

duce an algorithm that preserves distance-dependent connectivity as found in Proposition ??, but eliminates anisotropy in network connectivity by consecutively rewiring existing connections to new suitable targets.

**Definition 1.4.** Let  $G$  be an anisotropic geometric graph with  $|V(G)| = n$ . Then we define a rewiring of  $G$  to be probability space over  $G_\Phi^n$ , obtained by choosing for every edge  $e \in E(G)$  uniformly at random a potential new target  $t'(e)$  from the set  $M_e$  of all vertices that differ in their distance to  $s(e)$  less than  $\varepsilon$  from the distance of  $s(e)$  to  $t(e)$ ,

$$M_e = \{v \in V(G) \setminus s(e) \mid |d(s(e), v) - d(s(e), t(e))| < \varepsilon\}.$$

**Proposition 1.5.** *Preserves distance-connectivity.*

*Remark.* Partial rewiring.  $R_{\varepsilon, \eta}$

Here we choose  $\varepsilon = ??$ .

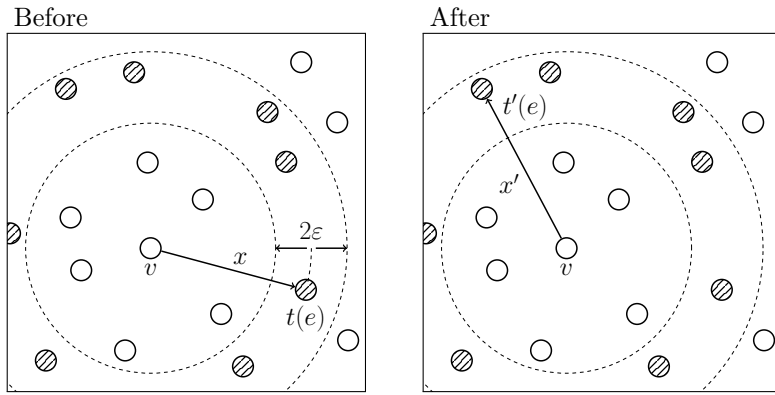


**Figure 1.10: Rewiring transforms anisotropic geometric graphs to networks with isotropic connectivity** For a given edge  $e$  with a distance  $x$  from its source vertex  $v$  to its target vertex  $t(e)$ , potential new targets (striped) are found in within a distance  $(x - \varepsilon, x + \varepsilon)$  of  $v$ . The rewired edge then projects from  $v$  to a new target  $t'(e)$ , randomly chosen from the set of vertices within in this range. Inter-vertex distance between  $v$  and  $t'(e)$  differs by less than  $\varepsilon$  from  $x$ , ensuring that for small  $\varepsilon$  the original distance-dependent connectivity is preserved.



## 1.6 ANISOTROPY MEASURE

In the last section a method to rewire an anisotropic geometric graph, such that was introduced. From an . In this chapter we introduce.. capturing ..

The  $G_{n,\Phi}$  be a geometric graph. Then, for every is the *preferred direction* and its length is

Mardia and Jupp (2000)

**Figure 1.11:** illustrate varying levels of anisotropy

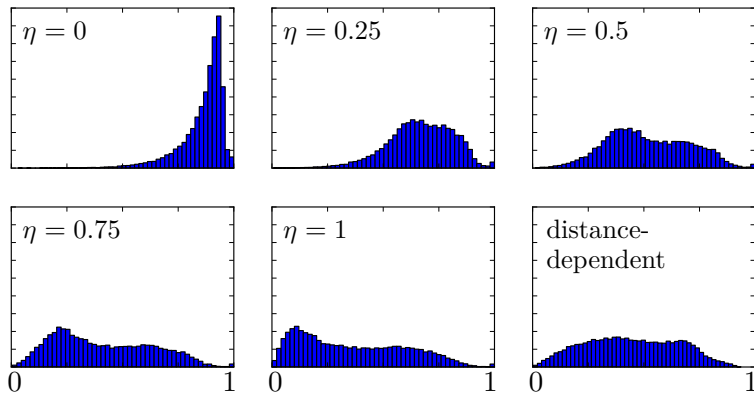


**Figure 1.12:** Isotropy distribution changes significantly through rewiring

## 1.7 SUMMARY AND DISCUSSION



## BIBLIOGRAPHY

---

- Braitenberg, Valentino and A Schüz (1998). *Cortex: Statistics and Geometry of Neuronal Connectivity*. 2nd ed. Berlin; New York: Springer.
- Debanne, Dominique (2004). Information processing in the axon. *Nature Reviews Neuroscience* 5.4, pp. 304–316.
- Feldman, ML (1984). Morphology of the neocortical pyramidal neuron. *Cerebral cortex, Vol 1, Cellular components of the cerebral cortex*. Ed. by Alan Peters and Edward G Jones. New York: Plenum Press, pp. 123–200.
- Ishizuka, Norio, Janet Weber, and David G Amaral (1990). Organization of intrahippocampal projections originating from CA3 pyramidal cells in the rat. *Journal of Comparative Neurology* 295.4, pp. 580–623.
- Jones, Eric, Travis Oliphant, Pearu Peterson, et al. (2001–). *SciPy: Open source scientific tools for Python*.
- Mardia, Kanti V. and Peter E. Jupp (2000). *Directional Statistics*. 2nd ed. John Wiley & Sons Ltd.
- Peixoto, Tiago (2014). *graph-tool - An efficient python module for manipulation and statistical analysis of graphs*.
- Perin, Rodrigo, Thomas K. Berger, and Henry Markram (2011). A synaptic organizing principle for cortical neuronal groups. *Proceedings of the National Academy of Sciences* 108.13, pp. 5419–5424. DOI: 10.1073/pnas.1016051108.
- Petersen, Carl C. H., Amiram Grinvald, and Bert Sakmann (2003). Spatiotemporal Dynamics of Sensory Responses in Layer 2/3 of Rat Barrel Cortex Measured In Vivo by Voltage-Sensitive Dye Imaging Combined with Whole-Cell Voltage Recordings and Neuron Reconstructions. *The Journal of Neuroscience* 23.4, pp. 1298–1309.
- Ramaswamy, Srikanth, Sean L Hill, James G King, Felix Schürmann, Yun Wang, and Henry Markram (2012). Intrinsic morphological diversity of thick-tufted layer 5 pyramidal neurons ensures robust and invariant properties of in silico synaptic connections. *The Journal of physiology* 590.4, pp. 737–752.
- Ramon, Y and S Cajal (1911). Histologie du systeme nerveux de l'homme et des vertebres. *Maloine, Paris* 2, pp. 153–173.
- Romand, Sandrine, Yun Wang, Maria Toledo-Rodriguez, and Henry Markram (2011). Morphological development of thick-tufted layer

- V pyramidal cells in the rat somatosensory cortex. *Frontiers in Neuroanatomy* 5.5. DOI: 10.3389/fnana.2011.00005.
- Ropireddy, Deepak, Ruggero Scorcioni, Bonnie Lasher, Gyorgy Buzsáki, and Giorgio A. Ascoli (2011). Axonal morphometry of hippocampal pyramidal neurons semi-automatically reconstructed after in vivo labeling in different CA3 locations. *Brain Structure and Function* 216.1, pp. 1–15. DOI: 10.1007/s00429-010-0291-8.
- Song, Sen, Per Jesper Sjöström, Markus Reigl, Sacha Nelson, and Dmitri B Chklovskii (2005). Highly Nonrandom Features of Synaptic Connectivity in Local Cortical Circuits. *PLoS Biol* 3.3, pp. 507–519. DOI: 10.1371/journal.pbio.0030068.
- Stepanyants, Armen and Dmitri B. Chklovskii (2005). Neurogeometry and potential synaptic connectivity. *Trends in Neurosciences* 28.7, pp. 387 –394. DOI: 10.1016/j.tins.2005.05.006.
- Stepanyants, Armen, Patrick R. Hof, and Dmitri B. Chklovskii (2002). Geometry and Structural Plasticity of Synaptic Connectivity. *Neuron* 34.2, pp. 275 –288. DOI: 10.1016/S0896-6273(02)00652-9.

## INDEX

---

anisotropic geometric  
graph, 7  
random graph model, 8  
apical dendrite, 4  
basal dendrite, 4  
neuro geometry, 2  
potential synapse, 2  
preferred direction, 15

Symbol	Description
$L$	Length
$Ma$	Mach number
$p$	Pressure